ISSN 1392-3196
Žemdirbystė=Agriculture, vol. 99, No. 3 (2012), p. 279–286
UDK 633.11:551.58

Impacts of climate change scenarios on wheat yield determined by evapotranspiration calculation

Kourosh EHTERAMIAN[1], Ghorban NORMOHAMADI[1], Mohammad BANNYAN[2], Amin ALIZADEH[2]

[1]Islamic Azad University, Department of Agronomy, Science and Research Branch
Tehran, Iran
E-mail: Ehteramian_k@yahoo.com

[2]Ferdowsi University of Mashhad, Faculty of Agriculture
Mashhad, Iran

Abstract

Approximation of climate change effects on crop production could be biased depending upon the uncertainties in climate change scenarios, study location and methods of crop yield prediction. We evaluated the impact of climate change on wheat yield reduction percentage by determination of adjusted evapotranspiration. Climate projections of general circulation models (HadCM3) under three scenarios (SRA1B, SRES-A2 and SRES-B1) were employed in this study for different time periods (baseline (1961–1990), 2010–2039, 2040–2069, and 2070–2099) for Mashhad location. Statistical downscaling method was employed for developing quantitative relationship between large scale atmospheric variables (predictors) and local variables (observes). From the viewpoint of climatology, such parameters were also generated by a LARS-WG5 stochastic weather generator. The results showed that climate model had acceptable accuracy in prediction of climatic variables, especially maximum temperature. B1 scenario showed the highest rainfall amount, adjusted evapotranspiration and the lowest values of maximum temperature in contrast to other scenarios. In addition, A2 scenario showed the highest values of maximum and minimum temperatures and the lowest values of adjusted evapotranspiration in all study periods. Maximum wheat yield reduction was obtained under A2 scenario (57%) for the third time period (2070–2099) in comparison with the baseline. Nevertheless, B1 scenario showed minimum change in wheat yield for all time periods. In conclusion, wheat yield reduction process in Mashhad location is extremely related to climate scenario.

Key words: general circulation model, evapotranspiration, climate scenarios, wheat.

Introduction

Wheat (*Triticum aestivum* L.) is counted among the "big three" cereal crops, with over 600 million tons annual harvest. The total world harvest in 2007 was about 607 million tons compared with 652 million tons of rice and 785 million tons of maize (Shewry, 2009). Currently, about 95% of the wheat grown worldwide is bread wheat, and most of the remaining 5% being durum wheat (FAO statistics, 2008).

Climate change highly impacts agricultural production quantity and quality (Samadi et al., 2011). Climate change and global warming process will probably have direct impact on tropical and temperate regions and any other areas where high temperature or inadequate rain often limits crop productivity (Morison, Morecroft, 2006). Based on the projections of general circulation models (GCMs), the global average temperature is expected to increase between 2°C and 4.5°C during the current century (IPCC, 2007). The main constraint in assessing risk from climate change is the lack of long-term weather data and man's inability to predict the future weather (Abraha, Savage, 2006); however, various useful tools are being constantly developed (Bannayan, Hoogenboom, 2008).

Atmospheric GCMs are in use for seasonal forecasting by projecting a full set of meteorological variables at a sub-daily time step (Ines, Hansen, 2006). All general circulation models, which are rooted in physical principles, are assumed to be permanent. They often differ in the simplifying assumptions (e.g., regression functions) and parameterization methods employed to make them computationally efficient (Arnell et al., 2004). GCMs contain significant uncertainties and there are different models and scenarios such as, A2 and B2 for predicting future climate in different situations (Wilby et al., 1999).

Stochastic downscaling approaches typically involve modifying the parameters of conventional weather generators such as WGEN or LARS-WG. Climate change scenarios are generated stochastically using revised parameter sets scaled in direct proportion to the corresponding parameter changes in a GCM. The main advantage of the technique is that it can exactly reproduce many observed climate statistics and has been widely used, particularly for agricultural impact assessment (Samadi et al., 2011).

The A2 scenario is one of the most extreme scenarios, with carbon emission rising from about 10 Gt at present to over 25 Gt in 2100 (medium to high carbon

emission) (Prudhomme et al., 2010). This scenario describes the maximum potential impact of future climate on specific dynamics. The B2 scenario is more optimistic (low to medium carbon emission) counterpoint (Hewitson, Crane, 1996). GCM projections can be used to provide weather data for future-oriented crop simulations (Reddy, Pachepsky, 2000).

Evapotranspiration is one of the major apparatus of the hydrologic cycle and its precise estimation is of paramount importance for many studies such as hydrologic water balance, irrigation system plans and management, crop yield simulation, and water resources planning and management (Archana, Shrivastava, 2010). Using crop coefficient for crop evapotranspiration (ET_c) calculation was introduced by Doorenbos and Pruitt (1977), whereby the impact of the climate on crop water supplies is given by the reference evapotranspiration (ET_o) and the effect of the specific crop characteristics by the crop coefficient (K_c).

The K_c is the ratio of the crop ET to the reference ET and represents the integration of the effects of a series of characteristics that discriminate the crop from reference grass (Miranda et al., 2006). The FAO56-PM model, which fits in thermodynamic and aerodynamic aspects, has been established to be a moderately accurate method in both humid and arid climates (Yin et al., 2008). Crop evapotranspiration showed direct correlation with various crops' production (Ko, Piccinni, 2009).

The main objective of this study was to evaluate wheat yield reduction under climate change process by calculating wheat evapotranspiration with two different general circulation models (IPCM4 and HadCM3) under three different scenarios (A1B, A2 and B1) in the northeast of Iran. We hypothesize that wheat yield will be reduced under climate change due to more evapotranspiration in response to increasing temperature.

Materials and methods

Study area. The study was conducted at Mashhad plain in 2011. Mashhad plain, covering 16500 km^2, is located in the northeast of Iran, Khorasan province. This region is located between 35°40′ and 36°3′ north latitude and 58°2′ and 60°8′ east longitude. The climate regime of this plain is cold and arid. Mean annual temperature is 13.6°C and the average annual precipitation is 220 mm (IMO, 2009). In the mountainous part of Khorasan province, the annual precipitation exceeds 230 mm with the record of 324 mm at the highest location.

Data sets. Daily climate data, including maximum and minimum temperature (ºC) and precipitation (mm), were obtained for the period of 1961–1990 from Mashhad meteorological station. Two GCMs and three scenarios were employed in this research. The GCM models included the Institute of Pierre Simon Laplace (IPCM4) and United Kingdom Met Office Hadley Centre (HadCM3) (Mitchell et al., 1995) and scenarios were SRA1B, SRES-A2 and SRES-B1.

LARS-WG is a stochastic weather generator based on the series approach (Semenov, Brooks, 1999). LARS-WG produces synthetic daily time series of maximum and minimum temperature, precipitation and solar radiation. LARS-WG applies observed daily weather data for a given site to compute a set of parameters for probability distributions of weather variables as well as correlations between them (Semenov, Brooks, 1999). In this study, this model was used to produce daily climate variables as one stochastic set of data for a growing season for each projection period which is required for ET_o calculation. Climatic data including maximum and minimum temperature and precipitation of Khorasan province were generated for four projection periods (1961–1990 (baseline), 2010–2039, 2040–2069, and 2070–2099).

Climate model validation. Several criteria were calculated to quantify the difference between simulated and observed data. The root mean-squared error (RMSE) is computed to measure the coincidence between measured and simulated values for baseline of climatic model as follows:

$$RMSE = \frac{100}{\bar{O}}\sqrt{\frac{\sum_{i=1}^{n}(P_i - O_i)^2}{n}} \quad (1),$$

where P and O are simulated and observed data, respectively, in addition $\bar{O}$ is the mean of observed data and *n* is the number of observations.

Yield reduction factor. Yield reduction factor was obtained by the following equation (Allen et al., 1998):

$$\left[1 - \frac{Y_a}{Y_m}\right] = K_y\left[1 - \frac{ET_{cadj}}{ET_c}\right] \quad (2),$$

where Ya, Ym, Ky, ET_{cadj} and ET_c are actual yield of the crop (kg ha^{-1}), maximum yield in absence of environmental or water stresses, yield response factor, potential crop evapotranspiration and actual crop evapotranspiration, respectively.

Crop evapotranspiration under soil water stress conditions (ET_{cadj}). The ET_{cadj} (mm d^{-1}) was estimated as (Allen et al., 1998):

$$ET_{cadj} = K_S \times K_C \times ET_O \quad (3).$$

ET_{cadj} values calculated for growth season of wheat according to common sowing date (early October) and growing season length (180 days) of this region.

Water stress coefficient (K_s). The effects of soil water stress on crop ET are described by reducing the value for the crop coefficient. This is accomplished by multiplying the crop coefficient (K_c) by the water stress coefficient (K_s). The water stress coefficient (K_s) was determined as (Allen et al., 1998):

$$K_{s,i} = (TAW_i - D_{r,i})/(TAW_i - RAW_i) \quad (4),$$

where $K_{s,i} = 1$ when $D_{r,i}$ is smaller than or equal to readily available water (RAW_i), otherwise $K_s < 1$. For a given day, total available water (TAW_i) is determined from the daily crop rooting depth ($Z_{r,i}$), field capacity (FC) and permanent wilting point (PWP) for soil at the rooting depth. The RAW_i is then expressed as $_pTAW_i$, where p is the soil depletion factor that represents the fraction of TAW_i that can be depleted from the root zone before water-stress occurs.

Crop coefficient (K_c). Crop development takes place in four stages as initial stage, crop development stage, mid season stage and late season stage. The length of each development stage was determined from local information and the length of growing period of crop was

considered based on farmers' practice in the study area (Gontia, Tiwari, 2009). Monthly crop coefficient (K_c) was estimated using the guidelines given in irrigation and drainage paper FAO-56 (Allen et al., 1998) for wheat crop depending upon the stage of growth and adjusting by the following equations:

$$K_{cmid} = K_{cmid(tab)} + [0.04(u_2 - 2) - 0.004(RH_{\min} - 45)]\left(\frac{h}{3}\right) \times 0.3 \quad (5),$$

$$K_{cend} = K_{cend(tab)} + [0.04(u_2 - 2) - 0.004(RH_{\min} - 45)]\left(\frac{h}{3}\right) \times 0.3 \quad (6),$$

where $K_{cmid(tab)}$ and $K_{cend(tab)}$ are the tabulated values for K_{cmid} and K_{cend} respectively in Table 12 of FAO-56 (Allen et al. 1998). RH_{min} is the mean value for daily minimum relative humidity during the midseason growth stage (%), for $20\% \le RH_{min} \le 80\%$, and h is mean plant height during the mid-season stage (m) for 0.1 m < h < 10 m (Gontia, Tiwari, 2009).

Reference evapotranspiration (ET_o). Potential evapotranspiration for each day was calculated using the FAO (Food and Agricultural Organization of the United Nations) modified form the Penman-Monteith equation (Allen et al., 1998):

$$ET_o = \frac{0.408\Delta(R_n - G) + \gamma\left(\frac{900}{T+273}\right) \times u_2 \times (e_s - e_a)}{\Delta + \gamma(1 + 0.34 \times u_2)} \quad (7),$$

where ET_o is reference evapotranspiration (mm day^{-1}), Δ is slope of the vapour pressure curve, R_n is net radiation at the surface (MJ $m^{-2}d^{-1}$), G is soil heat flux density (MJ $m^{-2}d^{-1}$), g is psychrometric constant, T is mean daily air temperature at 2 m height, u_2 is wind speed at 2 m height, e_s is the saturated vapour pressure and e_a is the actual vapour pressure (kPa). Daily values of total solar radiation at the earth's surface (Rs) were estimated using the procedure of Hargreaves and Samani (1982) and as subsequently modified by Allen (1997). Extraterrestrial solar radiation (R_a) (MJ $m^{-2}d^{-1}$) was first calculated at the top of the earth's atmosphere for each study day based on latitude, longitude, and the solar constant (Allen, 1997). Then, R_s was calculated using the following equation:

$$R_S = K_{Rs}(1 + 2.7 \times 10^{-15} \times Alt) \times (T_{\max} - T_{\min})\, 0.5 \times R_a \quad (8),$$

where Alt is the altitude (m) and K_{Rs} is an empirical coefficient set at 0.16 (Hargreaves, Samani, 1982). Clear-sky solar radiation (R_{so}) was calculated by the following equation (Allen et al., 1998):

$$R_{SO} = (0.75 + 2 \times 10^{-5} \times z) R_a \quad (9),$$

where z is the station elevation above sea level (m).

In addition, net shortwave radiation (R_{ns}) was obtained by the following formula (Allen et al., 1998):

$$R_{ns} = (1 - \alpha) R_S \quad (10),$$

in which α is the albedo or canopy reflection coefficient, which is 0.23 for the hypothetical grass reference crop.

Net longwave radiation (R_{nl}) which is the rate of longwave energy emission is proportional to the absolute temperature of the surface raised to the fourth power, calculated as follows (Allen et al., 1998):

$$R_{nl} = \sigma\left[\frac{T_{\max,K^4} + T_{\min,K^4}}{2}\right] \times (0.34 - 0.14\sqrt{e_a}) \times \left(1.35\frac{R_S}{R_{SO}} - 0.35\right) \quad (11),$$

where σ is Stefan-Boltzmann constant (4.903×10^{-9} MJ K^{-4} $m^{-2}d^{-1}$) and finally, net radiation at the surface (R_n) obtained by differences between R_{ns} and R_{nl}.

Vapour pressure deficit (es – ea). Calculation of VPD was based on estimates of the differences between the average daily saturated water vapour pressure (e_s) and the actual water vapour pressure (e_a). Estimation of actual vapour pressure (e_a) can be obtained by assuming that dewpoint temperature (T_{dew}) is near the daily minimum temperature (T_{min}) using the following equation (Allen et al., 1998):

$$e_a = 0.611\exp\left[\frac{17.27T_{dew}}{T_{dew} + 237.3}\right] \quad (12).$$

Saturated water vapour pressure (e_s) was calculated according to saturation vapour pressure at minimum and maximum temperature (Allen et al., 1998):

$$e^o(T_{\max}) = 0.611\exp\left[\frac{17.27T_{\max}}{T_{\max} + 237.3}\right] \quad (13),$$

$$e^o(T_{\min}) = 0.611\exp\left[\frac{17.27T_{\min}}{T_{\min} + 237.3}\right] \quad (14),$$

$$e_S = \frac{e^o(T_{\max}) + e^o(T_{\min})}{2} \quad (15).$$

Results and discussion

Climate model. The accurate estimation of weather variables such as temperature and precipitation in baseline time period might indicate correctness of downscaling models in climate change studies (Viglizzo et al., 1997). Climate downscaling model illustrated utmost accuracy projection (RMSE = 1.7%) in maximum temperature simulation in comparison with baseline (Fig. 1 b). However, minimum temperature simulation showed more than 15% (RMSE = 19%) difference between simulated and observed values (Fig. 1 a). Precipitation simulation precision (RMSE = 11%) was less than maximum temperature (Fig. 1 c). Bannayan et al. (2011) reported that minimum temperature of Mashhad showed high fluctuation and sharply increased during the last 40 years (1960–2000). It can be concluded that unbalanced trend of minimum temperature is the main reason of climate poorer accuracy in prediction of this climatic variable compared to maximum temperature and precipitation. Kousari and Asadi Zarch (2011) showed a significantly increasing trend in the annually minimum and mean temperatures.

Climatic variables. The results showed that A1B scenario indicated the highest annual precipitation rate across all study scenarios for 2010–2039 (382 mm) and 2070–2099 (343 mm) time periods (Fig. 2). However, the highest amount of annual precipitation was obtained under B1 scenario (377 mm) for 2040–2069 time period

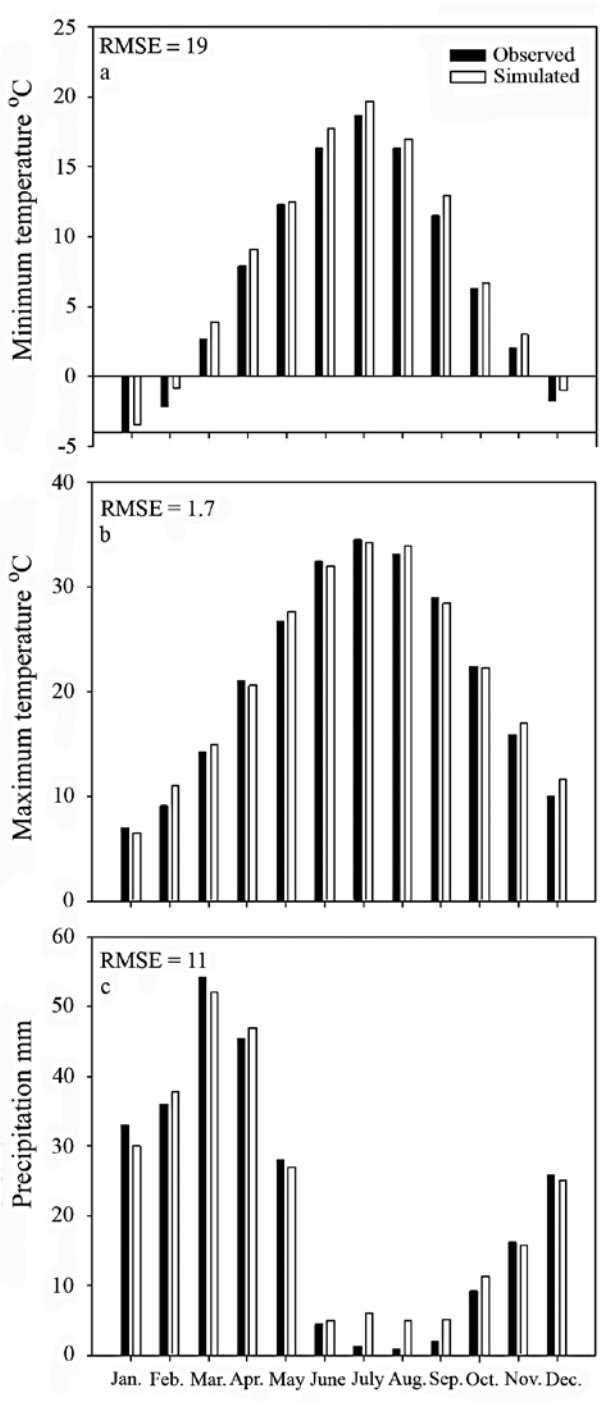

Figure 1. Comparison of simulated and observed climatic parameters for Mashhad plain

(Fig. 2). As expected, A1B and A2 scenarios showed the highest values of maximum and minimum temperatures in all time periods in contrast to B1 scenario (Figs 3 and 4). Prudhomme et al. (2010) reported that mean annual warming under A1B and A2 scenarios was higher than under B1 scenario in future climate change conditions.

B1 scenario showed the lowest values of maximum and minimum temperatures (average) across all study scenarios and time periods especially in growth period of wheat except minimum temperature average for 2070–2099 time period in Mashhad location (Figs 3 and 4). B1 scenario is a highly positive scenario; however, population growth is the same as for A1 (pessimistic scenario). On the other hand, development rate will get a much more environmentally sustainable projection with global-scale assistance and instruction (Arnell, 2004). Also, clean and efficient technologies are established. The emphasis is on global solutions to achieving economic, social and environmental sustainability (Arnell et al., 2004).

Adjusted evapotranspiration (ET_{cadj}) and yield redaction percentage. According to the adjusted evapotranspiration calculation results, B1 scenario (161 mm as cumulative ET_{cadj}) showed the highest average values of ET_{cadj} for all time periods across all performed scenarios (Fig. 5). There was no significant difference between A1B and A2 scenarios in ET_{cadj} values (less than 4 mm) across all study periods (Fig. 5). Second time period (2040–2069) indicated the highest cumulative values of ET_{cadj} (156 mm) across different time periods (Fig. 5). ET values have direct relationship with temperature, specifically with the maximum temperature (Galleguillos et al., 2011). Moreover, evaporation from crop surface decreased due to the increasing rate of stomata closure under higher temperature conditions (Mu et al., 2011). Therefore, ET_{cadj} values are significantly lower under A2 and A1B scenarios.

The highest wheat yield reduction percentage compared to baseline was gained under the A2 scenario across 2040–2069 (38%) and 2070–2099 (57%) time periods (Fig. 6). However, B2 scenario showed less than 10% yield loss in all studied time periods. In addition, A1B indicated more than 10% yield reduction (12%) in 2040–2069 time periods (Fig. 6). Yield reduction of wheat was simulated under future climate change in Iran to range from 22% to 32% for year 2050 (Koocheki, Kamali, 2010). They reported that reduction of wheat yield occurred due to increasing evapotranspiration. Some reports confirmed direct and positive correlation between ET_{cadj} and different crops' production (Novick et al., 2009).

It seems that the main reason of lower wheat yield reduction under B1 scenario in comparison with baseline was higher values of ET_{cadj} in that scenario. There were no considerable differences in ET_{cadj} values between A2 and A1B scenarios in 2070–2099 time periods. However, ET_{cadj} values were extremely low (44 mm) during the reproductive phase (120–180 days) of wheat under A2 scenario for that time period compared to other scenarios. Increasing of temperature led to the increase of development rate of crop and decrease of growth period (Bannayan et al., 2011) which resulted in yield reduction. Consequently, higher yield reduction of wheat in A2 scenario resulted from higher temperature and short growth period in this scenario. On the other hand, increasing of temperature in A1B scenario was higher than in A2 scenario but ET_{cadj} values under A2 scenario were lower during the reproductive phase than in A1B scenario, therefore, in essence, yield reduction in A2 scenario was the highest due to high temperature and low ET_{cadj} especially in reproductive phase. Our results showed that wheat yield will be reduced by 6% to 57% in future climate change compared to baseline and it will affect rural population since wheat is an economically strategic crop for farmers. Therefore, attention to management approach for decreasing adverse effects of changing climate is necessary which will result in higher sustainability in rural areas.

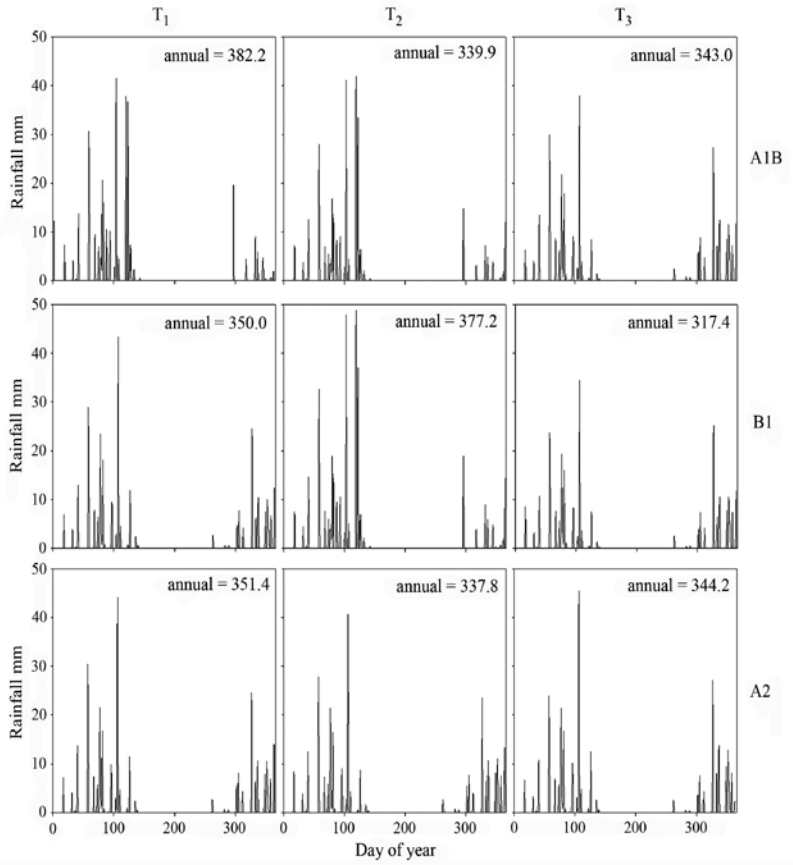

Figure 2. Precipitation fluctuations under A1B, A2 and B1 scenarios for different time periods (T1 = 2010–2039, T2 = 2040–2069 and T3 = 2070–2099)

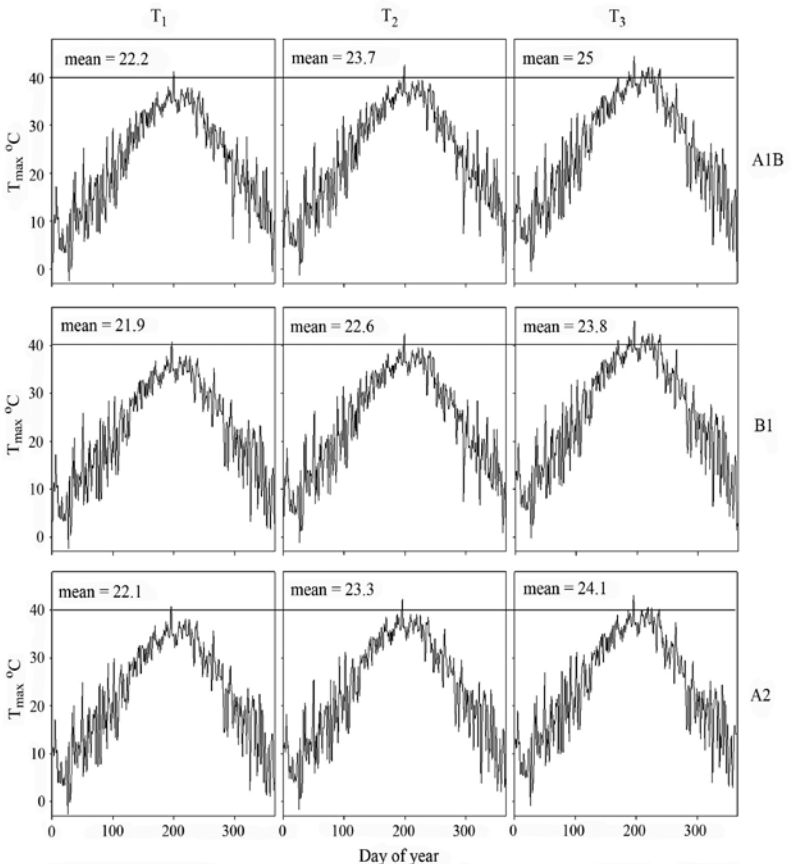

Figure 3. Maximum temperature fluctuations under A1B, A2 and B1 scenarios in different time periods (T1 = 2010–2039, T2 = 2040–2069 and T3 = 2070–2099)

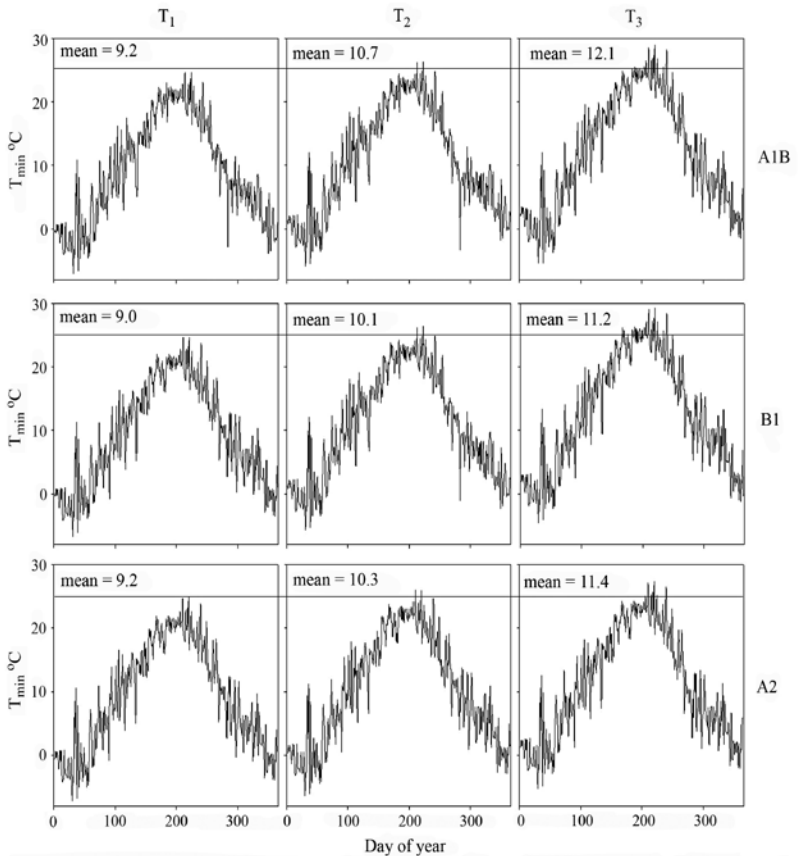

Figure 4. Minimum temperature fluctuations under A1B, A2 and B1 scenarios in different time periods (T1 = 2010–2039, T2 = 2040–2069 and T3 = 2070–2099)

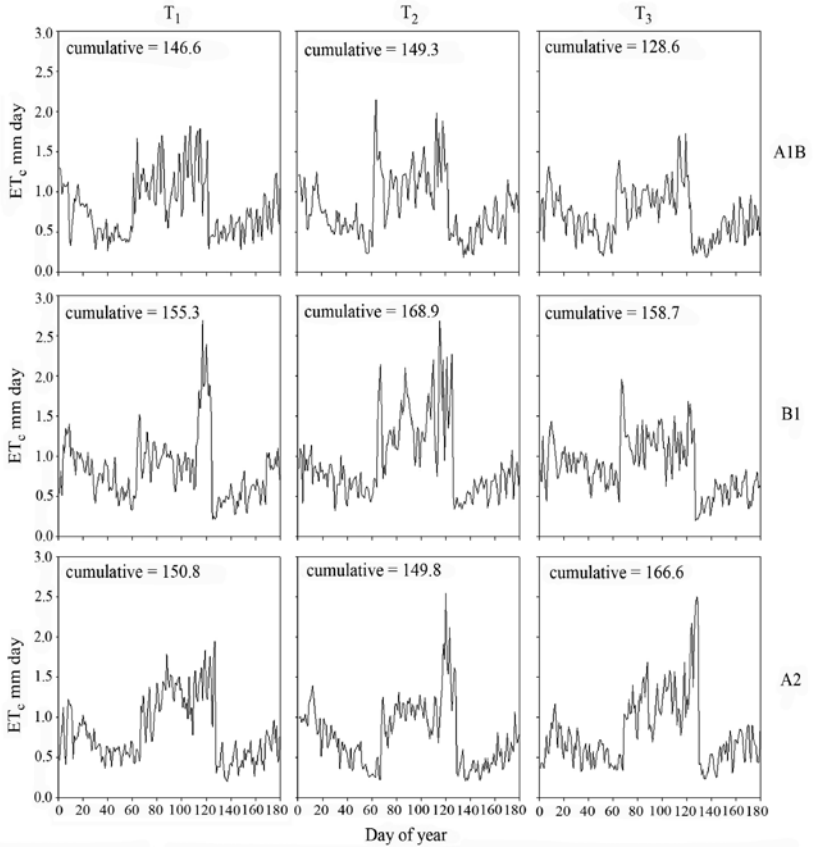

Figure 5. ET_{cadj} fluctuations during growth period of wheat under A1B, A2 and B1 scenarios in different time periods (T1 = 2010–2039, T2 = 2040–2069 and T3 = 2070–2099)

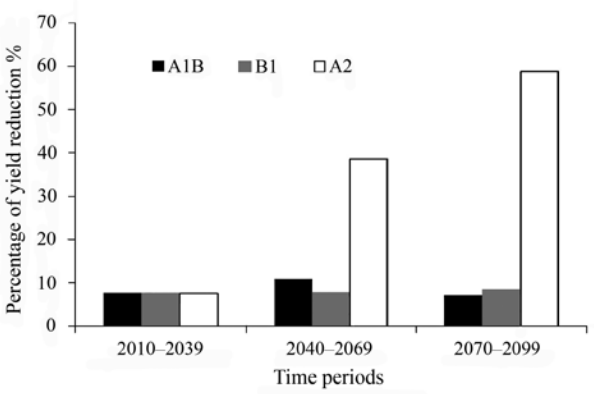

Note. Avearge wheat yield for baseline was considered 3900 kg ha^{-1}.

Figure 6. Yield reduction percentage of wheat under A1B, A2 and B1 scenarios in different time periods (T1 = 2010–2039, T2 = 2040–2069 and T3 = 2070–2099) for Mashhad plain compared to baseline (1961–1990)

Conclusions

1. The results showed that LARS-WG generated climatic parameters with high accuracy for baseline period and we used it for simulation of climate conditions in the future.

2. Based on the values of RMSE, maximum temperature was estimated more accurately as compared to the estimation of minimum temperature and precipitation.

3. B1 scenario showed the most optimistic situation for future climate due to the highest values of precipitation and lowest values of maximum temperatures in all study periods.

4. Wheat yield was reduced under all climate change scenarios and times, and this yield reduction was different based on various scenarios.

5. As observed, B1 scenario showed the lowest average yield reduction percentage compared to other scenarios across the time periods because the averages of maximum and minimum temperatures were lower in B1 scenario in comparison with A2 and A1B scenarios.

6. A2 scenario indicated the highest decrease in wheat yield for all study periods, especially for 2070–2099 time period, and also the critical phase of wheat growing season due to higher evapotranspiration and average of maximum temperature occurred under these conditions.

7. Wheat yield reduction trend is tremendously related to population growth and changing sustainable technologies. Generally, reduction of wheat yield was approximated under climate change in future which will affect economic and social issues in Mashhad location, where most farmers are smallholders and the local economy highly dependents on cultivation of wheat. As a result, management approaches such as shifting planting date, applying appropriate irrigation and using appropriate varieties are needed to reduce adverse effects of climate change. Based on the above mentioned and the highest yield reduction of wheat under A2 scenario, it could be concluded that A2 scenario will remarkably affect farmers' lives in terms of economic and social issues as compared with other scenarios. This will in turn lead to the increase of migration of rural population towards urban areas or to non-agriculture livelihood opportunities and it can be expected that B1 scenario will have a smaller effect on these issues.

Received 18 01 2012
Accepted 08 06 2012

Reference

Abraha M. G., Savage M. J. Potential impacts of climate change on the grain yield of maize for the midlands of KwaZulu-Natal, South Africa // Agriculture, Ecosystems and Environment. – 2006, vol. 115, p. 150–160

Allen R. G. Self-calibrating method for estimating solar radiation from air temperatures // Journal of Hydrologic Engineering. – 1997, vol. 2, p. 56–67

Allen R. G., Pereira L. S., Dirk R., Smith M. Crop evapotranspiration guidelines for computing crop water requirements / FAO Irrigation and Drainage Paper No. 56. – Rome, Italy, 1998, p. 103–156

Archana C., Shrivastava R. K. Reference crop evapotranspiration estimation using Artificial Neural Networks // International Journal of Engineering Science and Technology. – 2010, vol. 2, No. 9, p. 4205–4212

Arnell N. W. Climate change and global water resources: SRES emissions and socio-economic scenarios // Global Environmental Change. – 2004, vol. 14, p. 31–52

Arnell N. W., Livermore M. J. L., Kovats S., Nicholls R., Levy P., Parry M. L., Gaffin S. R. Climate and socio-economic scenarios for global-scale climate change impacts assessments: characterising the SRES storylines // Global Environmental Change. – 2004, vol. 14, p. 3–20

Bannayan M., Eyshi Rezaei E., Mohamadian A., Alizadeh A. Detecting possible trends of climate variables for conditions in northeast of Iran // International Journal of Climatology. – 2011 (submitted)

Bannayan M., Hoogenboom G. Weather analogue: a tool for real-time prediction of daily weather data realizations based on a modified k-nearest neighbor approach // Environmental Modelling and Software. – 2008, vol. 3, p. 703–713

Doorenbos J., Pruitt W. O. Guidelines for predicting crop water requirements / FAO Irrigation and Drainage Paper No. 24. – Rome, Italy, 1977, p. 53–82

FAO statistics. – 2008. <http://faostat.fao.org> [accessed 12 08 2012]

Galleguillos M., Jacob F., Prevot L., French A., Lagacherie P. Comparison of two temperature differencing methods to estimate daily evapotranspiration over a Mediterranean vineyard watershed from ASTER data // Remote Sensing of Environment. – 2011, vol. 115, iss. 6, p. 1326–1340

Gontia N. K., Tiwari K. N. Estimation of crop coefficient and evapotranspiration of wheat (*Triticum aestivum*) in an irrigation command using remote sensing and GIS // Water Resource Management. – 2009, vol. 24, p. 1399–1414

Hargreaves G. H., Samani Z. A. Estimating potential evapotranspiration // Journal of Irrigation and Drainage Engineering. – 1982, vol. 108, p. 225–230

Hewitson B. C., Crane R. G. Climate downscaling Techniques and applications // Climatic Research, vol. 7, p. 85–95

Ines A. V. M., Hansen J. W. Bias correction of daily GCM rainfall for crop simulation studies // Agriculture and Forest Meteorology. – 2006, vol. 138, p. 44–53

IPCC. Climate Change 2007: The Physical Science Basis / Contribution of Working Group I to the 4th Assessment Report of the Intergovernmental Panel on Climate Change. – Cambridge, UK, New York, USA, 2007, p. 24–57

IRIMO. Tehran, Iran, 2009. <http://www.irimo.ir> [accessed 20 09 2011]

Ko J., Piccinni G. Corn yield responses under crop evapotranspiration-based irrigation management // Agricultural Water Management. – 2009, vol. 96, p. 799–808

Koocheki A., Kamali G. Climate change and wheat production in Iran // Iranian Journal of Field Crops Research. – 2010, vol. 8, p. 508–520
Kousari M. R., Asadi Zarch M. A. Minimum, maximum, and mean annual temperatures, relative humidity, and precipitation trends in arid and semi-arid regions of Iran // Arabian Journal of Geosciences. – 2011, vol. 4, p. 907–914
Miranda F. R., Gondim R. S., Costa C. A. G. Evapotranspiration and crop coefficients for tabasco pepper (*Capsicum frutescens* L.) // Agricultural Water Management. – 2006, vol. 82, p. 237–246
Mitchell J. F. B., Johns T. C., Gregory J. M., Tett S. Climate response to increasing levels of greenhouse gases as sulphate aerosols // Nature. – 1995, vol. 376, p. 501–504
Morison J. I. L., Morecroft M. D. Plant growth and climate change (Biological sciences series). – Oxford, UK, 2006, 213 p.
Mu Q., Zhao M., Running S. W. Improvements to a MODIS global terrestrial evapotranspiration algorithm // Remote Sensing of Environment. – 2011, vol. 115, p. 1781–1800
Novick K. A., Oren R., Stoy P. C., Siqueira M. B. S., Katul G. G. Nocturnal evapotranspiration in eddy-covariance records from three co-located ecosystems in the Southeastern U.S.: implications for annual fluxes // Agricultural and Forest Meteorology. – 2009, vol. 149, p. 1491–1504
Prudhomme C., Wilby R. L., Crooks S., Kay A. L., Reynard N. S. Scenario-neutral approach to climate change impact studies: application to flood risk // Journal of Hydrology. – 2010, vol. 390, p. 198–209
Reddy V. R., Pachepsky Y. A. Predicting crop yields under climate change conditions from monthly GCM weather projections // Environmental Modelling and Software. – 2000, vol. 15, p. 79–86
Samadi S., Ehteramian K., Sarraf B. S. SDSM ability in simulate predictors for climate detecting over Khorasan province // Procedia: Social and Behavioral Sciences. – 2011, vol. 19, p. 741–749
Semenov M. K., Brooks R. J. Spatial interpolation of the LARS-WG stochastic weather generator in Great Britain // Climate Research. – 1999, vol. 11, p. 137–148
Shewry P. R. Wheat // Journal of Experimental Botany. – 2009, vol. 60, p. 1537–1553
Viglizzo E. F., Roberto Z. E., Lertora F., Gay E. L., Bernardos J. Climate term and land-use previous change term in field-crop ecosystems of Argentina // Agriculture Ecosystems and Environment. – 1997, vol. 66, p. 61–70
Wilby R. L., Hay L. E., Leavesley G. H. A comparison of downscaled and raw GCM output: implications for climate change scenarios in the San Juan River basin, Colorado // Journal of Hydrology. – 1999, vol. 225, p. 67–91
Yin Y., Wu S., Zheng D., Yang Q. Radiation calibration of FAO56 Penman-Monteith model to estimate reference crop evapotranspiration in China // Agricultural Water Management. – 2008, vol. 95, p. 77–84

ISSN 1392-3196
Žemdirbystė=Agriculture, vol. 99, No. 3 (2012), p. 279–286
UDK 633.11:551.58

Žieminių kviečių derlius pagal klimato kaitos scenarijus skaičiuojant evapotranspiraciją

K. Ehteramian[1], G. Normohamadi[1], M. Bannyan[2], A. Alizade[2]

[1]Irano islamiškasis Azad universitetas, Agronomijos fakultetas, Mokslo ir tyrimų skyrius
[2]Irano Mashhado Ferdowsi universitetas, Žemės ūkio fakultetas

Santrauka

Klimato kaitos įtakos augalininkystei nustatymas gali būti tendencingas, priklausomai nuo klimato pokyčių scenarijų, tyrimų vietos ir augalų derliaus prognozavimo metodų neapibrėžtumo. Tyrimo metu vertinta klimato kaitos įtaka derliaus sumažėjimo procentui, nustatant pakoreguotą evapotranspiraciją. Taikytos bendrų cirkuliacijos modelių (HadCM3) klimato projekcijos pagal tris scenarijus (SRA1B, SRES-A2 ir SRES-B1) Mashhad vietovėje įvairiais laikotarpiais (pradinis taškas – 1961–1990 m.): 2010–2039, 2040–2069 ir 2070–2099 m. Kuriant kiekybinį ryšį tarp didelio mastelio atmosferos kintamųjų ir vietinių kintamųjų, taikytas statistinis *downscaling* metodas. Dienos klimatologiniai parametrai buvo kuriami naudojant tikimybinį (stochastinį) oro generatorių LARS-WG 5. Rezultatai parodė, kad klimato modelis pakankamai tiksliai prognozavo klimato kintamuosius, ypač maksimalią temperatūrą. Skirtingai nei kiti scenarijai, B1 scenarijus parodė didžiausią kritulių kiekį, pakoreguotą evapotranspiraciją ir mažiausias maksimalios temperatūros vertes. A2 scenarijus visais tyrimų laikotarpiais pademonstravo didžiausias maksimalios bei minimalios temperatūros vertes ir mažiausias pakoreguotos evapotranspiracijos vertes. Pagal A2 scenarijų kviečių derlius maksimaliai (57 %) sumažėjo 2070–2099 m. laikotarpiu, lyginant su pradiniu tašku. B1 scenarijus parodė minimalų kviečių derliaus pokytį visais laikotarpiais. Nustatyta, kad kviečių derliaus mažėjimo procesas Mashhad vietovėje yra labai glaudžiai susijęs su klimato kaitos scenarijumi.

Reikšminiai žodžiai: bendrasis cirkuliacijos modelis, evapotranspiracija, klimato kaitos scenarijai, kviečiai.